The Research of Medical Science Review
ISSN: 3007-1208 & 3007-1216 Volume 3, Issue 11, 2025

SYNERGISM OF ITRACONAZOLE AND CYCLOPHOSPHAMIDE NANOPARTICLES FOR BREAST CANCER; SYNTHESIS, CHARACTERIZATION AND CYTOTOXICITY

Fiza Anjum[*1], Muhammad Imran[2], Laiba Akhtar[3], Umeed Ullah Ghaznawi[4], Iqra Younas[5]

[*1,2,3,4]*University College of Pharmacy, University of the Punjab, Lahore*
[5]*Lahore College for Women University*

[*1]fizaanjum125@gmail.com, [2]mimrannasimi@gmail.com, [3]st.laibak@gmail.com,
[4]umeedjan06@gmail.com,[5]iqray1806@gmail.com

DOI: https://doi.org/10.5281/zenodo.17810984

Keywords
Toxicity, Nanoparticles, Anticancer Activity

Article History
Received: 08 October 2025
Accepted: 15 November 2025
Published: 29 November 2025

Corresponding Author: *
Fiza Anjum

Abstract

Itraconazole has been known and used as anti-fungal drug for many years. But recently, clinical evidence has demonstrated the potential anticancer activity of itraconazole. Cyclophosphamide on the other hand, is a medication that particularly has been utilized in the management and treatment of several types of cancer since decades. In order to enhance the cancer immunotherapy response, the synthesis of nanoparticles has been suggested to be an effective way for smart targeted delivery of drug and to enhance the pharmacokinetic parameters of the drugs. Recently, Chitosan has been studied extensively due to its novel property of drug carrying capacity. This pertains to various advantages such as biodegradability, good biocompatibility and non-toxic properties. The purpose of this study is to evaluate the synergistic anti-cancer effects of chitosan loaded nanoparticles of itraconazole and cyclophosphamide on the breast cancer cells i.e.MCF-7. The ionic gelation method was used to produce Chitosan loaded nanoparticles of both Cyclophosphamide and Itraconazole. For the characterization of nanoparticles, the particle size analysis, FTIR and SEM were used. Furthermore, drug loading, entrapment efficiency and in-vitro dissolution profiles were evaluated.

The mean or average diameter of chitosan and Chitosan based Cyclophosphamide nanoparticles were in range 335.9nm and 213nm respectively, while 412nm for chitosan based Itraconazole nanoparticles. The deviation in the size of particles described that by addition of drug in affected their particle sizes. Average of the particle size for Chitosan NPs was slightly bigger than the CYP-CS-NPs whereas smaller than that of ITR-CS-NPs. Also, the efficiency regarding encapsulation of CYP-CS-NPs and ITR-CS-NPs was 62.4% and 98.79%, respectively (as per method). This is due to because the high polymer: drug ratio used that allowed the more drugs can be encapsulated inside core. The SEM analysis revealed that surface of drug-free chitosan nanoparticles; Cyclophosphamide-loaded chitosan nanoparticles and Itraconazole loaded nanoparticles were spherical along with some bands. Kinetic parameters like release profiles (in-vitro), regarding CYP-CS-NPs and ITR-CS-NPs showed good sustained-release up to 50% at 8hours. ITR showed sustaining properties due to

its bigger size and better encapsulation efficiency. The cytotoxic-studies established that ITR-CS-NPs possess anti-cancer activity the against MCF7 cell-lines and can be repurposed for it's used along with cyclophosphamide for the effective treatment of Breast Cancer.

INTRODUCTION

Cancer is the second most leading cause of mortality, accounting for over 10 million deaths in year 2020 (WHO, 2022)(Weinberg, 1996). Several gene mutations are involved in cancer pathogenesis, leading to the abnormal cell growth (Hassanpour, 2017). Impaired gene function and altered gene expression are two most common characteristics of cancer (Henrich, 2007). In men, the type of cancer in highest percentage includes Urinary bladder, prostate, rectum and colon respectively. However, in females, the percentage of cancer prevails greater in bronchus, breast, thyroid, lungs and uterine (Miller, et al., 2016). (Hegde & Chen, 2020) While in children, blood cancer and lymph node cancer are most frequent (Schottenfeld & Fraumeni Jr, 2006); (Yoo & Shin, 2003).

1.1 Breast Carcinoma

Breast cancer has been one of the most common cancers which typically affects women over 50 years old as well as younger people with AFAB (Hoadley, et al., 2016). Men and AMAB individuals can also develop breast cancer. Around 30% of all newly diagnosed cancers are breast cancer (Breast Cancer Facts and Statistics, 2024) (Breast Cancer Hormone Receptor Status).

1.2 Pathophysiology

Breast cancer is a heterogeneous disease with various polymorphic genomic and pathological alterations. Tumor cells experience genetic, epigenetic and microenvironmental pressures leading to tumor heterogeneity (Danhausen, Phillippi, & McCance, 2019). Risk factors include reproductive factors (nulliparity, pre-, mid-, or post-partum cancer), familial syndromes, lifestyle, and environmental exposures such as radiation and hormones. Carcinogens including alcohol, contraceptives, and steroidal hormones in menopausal therapy, X- and γ-radiation contribute to breast cancer development.

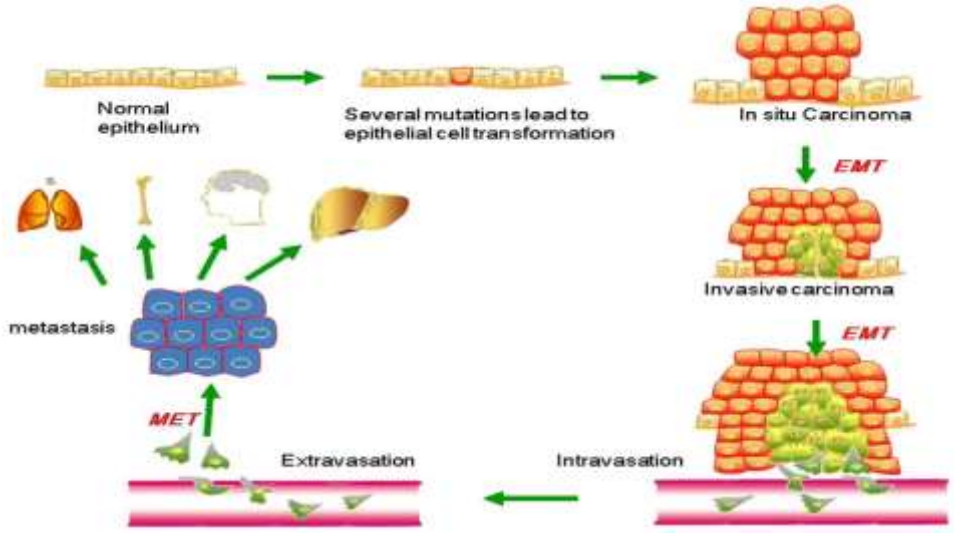

Figure1.1 Breast Cancer Progression (Liu, Gu, Shan, & Sang, 2016)

*[EMT= epithelial-to-mesenchymal transition, MET= mesenchymal-epithelial.]

Normal epithelial cells undergo malignant transformation. Invasive carcinoma arises from clonal expansion, with some cells undergoing epithelial-mesenchymal transition (EMT) to enter vascular or lymphatic structures. Extravasated cells use mesenchymal-epithelial transition (MET) to form macro-metastases (Liu, Gu, Shan, & Sang, 2016). Most breast cancers are adenocarcinomas originating from the ductal epithelial layer as carcinoma in situ. LCIS arises from the duct-lobular unit (~84% of cases), while DCIS remains confined to lobules without invading the basal membrane (Winslow, 2012). The prime driver genes include MYC and HER2, whereas tumor-suppressor genes include TP53, BRSA1 and BRSA2. (Danhausen, Phillippi, & McCance, 2019)

1.3 Signs and Symptoms

Breast cancer may be asymptomatic or present as a small benign lump. Other signs include ulceration, reddish skin, nipple discharge, dimpling, axillary and skin retraction, palpable lymph nodes, and bone pain due to metastases. (Danhausen, Phillippi, & McCance, 2019)(Bhowmik, Laha, & Das, 2007)

Rising mortality and drug resistance necessitate more treatment options. Drugs such as alkylating agents, antimetabolites, aromatase inhibitors, anthracyclines, and antifungals have been repurposed for breast cancer (Abotaleb, et al., 2018) (Jonaid Ahmad Malik, et al., 2022),which can prove to be an excellent approach towards existing molecular targets (Jonaid Ahmad Malik, et al., 2022).

1.4 Nanotechnology

Researchers have found a potential strategy for delivering chemotherapy drugs, namely utilizing nanoparticles (NPs) as carriers (Rahman, Souto, Alam, & Beg, 2021). Nanotechnology is rapidly evolving, with over 150 clinical trials investigating NP-based carrier systems for cancer targeting. Liposomes, polymeric, solid, inorganic NPs, and micelles have been explored for oral, colorectal, and lung cancers (Sharma, Dave, Sanadya, Piush, & Sharma, 2010)

1.4.1 Nanoparticles

Nanoparticles are solid or liquid dispersions with sizes ranging from 10–10^3 nm. They can carry drugs by dissolution, encapsulation, or conjugation, creating nanospheres or nanocapsules. NP-mediated targeted drug delivery systems (NTDDS) can circulate chemotherapeutics and accumulate in tumor cells via selective receptor targeting (Mohanraj & Chen, 2006). Lipid-based NPs include solid lipid nanoparticles, liposomes, nanostructured lipid carriers, lipid-coated nanoparticles, micro-emulsions, nano-emulsions, phytosomes, and nanoassemblies (Mahmoud, Swidan, El-Nabarawi, & Teaima, 2022) NPs improve drug permeability, retention, stability, and targeting while reducing toxicity. Recent advances aim to target breast cancer stem cells (BCSCs) and improve outcomes for triple-negative breast cancer (TNBC) patients (Shreelaxmi Gavas, 2021). In short, nanotechnology has given the brand new perceptive for cancer treatment. (Oehler, Rajapaksha, & Albrecht, 2024)

1.4.2 Designing NTDDS

Designing NTDDS considers drug potency, NP size (typically 30–200 nm), and ligands for targeting. Chitosan, a natural polysaccharide from chitin deacetylation, enhances anti-cancer activity while minimizing effects on non-cancerous cells (Yedi Herdiana, 2023).

Chitosan nanoparticles can cross narrow junctions improving solubility, permeation, and pH-responsive drug release. Folate-conjugated chitosan NPs target adenocarcinoma cell lines via overexpressed folate receptors on the surface of MCF-7 (Deshmukh, Joshi, Vikhar, Khdabadi, & Tawar, 2022). Chitosan-loaded cyclophosphamide NPs combine the therapeutic effects of the drug with chitosan's benefits, improving bioavailability, drug loading, and release efficiency (Javad Sharifi-Rad, 2021) (Chun-Lan Li, 2022).

Alternative strategies include the repurposing of old drug molecules previously approved for other indications (Francesco Bertolini, 2015).

Itraconazole, an FDA-approved antifungal used clinically for decades, shows potential as an anti-cancer agent (X Wang, 2017).

1.5 Clinical Management of Breast Cancer in Pakistan

The burden of cancer is rising tremendously, but data regarding prevalence in Pakistan is limited. WHO reported a steady increase in cancer incidences, estimating over 83,000 cases (SKMH, 2018). Breast cancer is the leading cause of oncological deaths in Pakistan i.e. 48% deaths were caused by BC (Saeed, et al., 2019). As per report, 178,388 new cases of breast cancer were reported in Pakistan (Ali MM, 2020). Such high prevalence highlights the need for targeted interventions and cancer screening programs.

Awareness campaigns such as PINKtober by Pink Ribbon Pakistan, along with Pakistan's first dedicated breast cancer hospital, "Pink Ribbon Breast Cancer Trust Hospital," aim to reduce stigma and educate the public on early detection. Breast Cancer Awareness Day at Shaukat Khanum Memorial Hospital further promotes awareness and early treatment. (SKMH, 2018) (Saeed, et al., 2019)

A study investigating features, survival, and treatment patterns of breast cancer in Pakistan found that 23% of patients received neo-adjuvant chemotherapy, while 68.9% received adjuvant chemotherapy. Major predictors of overall survival included age, tumor size, stage, lymph node status, ER status, tumor grade, and treatment with hormonal therapy and radiation (Kumar, et al., 2016).

1.6 Rational of Study

Due to unsatisfactory outcomes of existing breast cancer treatments and high mortality, targeted cancer control interventions and early detection strategies are essential. Developing new molecules is costly and time-consuming, requiring extensive preclinical research, human testing, and FDA approval. Repurposing existing drugs offers an effective alternative by utilizing approved drugs for new therapeutic uses, conserving resources. Itraconazole, used for decades to treat fungal infections, has recently shown anti-cancer properties. Cyclophosphamide is an established anti-cancer drug for various malignancies. The repurposing of itraconazole nanoparticles, and their synergistic effects with cyclophosphamide nanoparticles against breast cancer, has not yet been explored in Pakistan.

2.0 Method for Literature Survey

Systematically examined studies from 2010 to December 2023 were those with the title "Synthesis, Characterization, and Cytotoxic Potential of CS-CYP and CS-ITR Nanoparticles against Breast Carcinoma Cell Line." Several research engines, including Google Scholar, PubMed, Science Direct, Medline, and Springer Link databases, were used to conduct the thorough literature evaluation. To conduct a thorough research, various key words, including "Cyclophosphamide nanoparticles," "Itraconazole nanoparticles," "Cyclophosphamide loaded Chitosan nanoparticles," "Itraconazole loaded Chitosan nanoparticles," "Cyclophosphamide nanoparticles for cancer treatment," and "Itraconazole nanoparticles for cancer treatment," were used. A manual Google search included a variety of publications, and several pieces cited a variety of references. A thorough search was done to ensure that the papers which were included in this chapter provided the most recent data on this research project.

Table 2.1: Inclusion Criteria for Literature Review

Sr No.	Inclusion criteria
1	Research articles on Cyclophosphamide and Itraconazole based nanoparticles published in between 2010 to 2023, with main focus on polymeric based CYP & ITR nanoparticles (Chitosan based)
2	Research Articles on in vitro and in vivo activities carried out using Cyclophosphamide loaded CS nanoparticles

3	Papers published showing in vitro and in vivo activities carried out using Itraconazole loaded CS nanoparticles
4	Articles employing Cyclophosphamide nanoparticles in cancer treatment
5	Articles employing Itraconazole nanoparticles in cancer treatment
6	Studies, reviews and abstracts and other literature published in national and international journals as well as the ones reported in scientific literature.

Table 2.2: Exclusion Criteria for Literature Review

Sr No.	Exclusion criteria
1	Publications before 2010
2	Studies devoid of clearly stated outcomes
3	Litrature published in a language other than English
4	Studies related to uses of CYP and ITR other than in cancer treatment
5	Studies including Cyclophosphamide and itraconazole in other forms besides nanoparticles

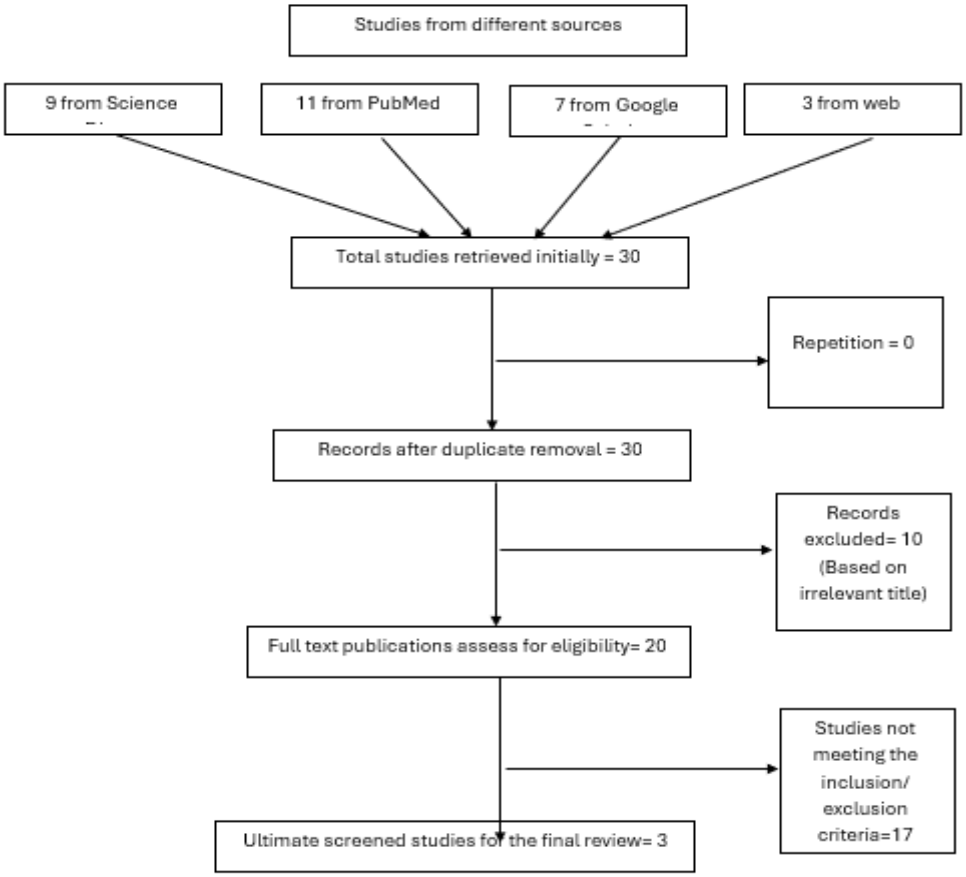

Table 2.3: List of Publications on CYP and ITR -loaded Chitosan Nanoparticles

Sr. No.	First Author Name / Year	Title	Type of Nanoparticles	Methodology	Results / Conclusion
1	(S.S.Agrawal & Sharma, 2017)	Anticancer Activity of Cyclophosphamide Nanoparticles against Ehrlich Ascites Carcinoma Cells Bearing Swiss Albino Mice	Cyclophosphamide loaded chitosan nanoparticles	The nanoparticles were prepared by ionic gelation process	The study showed that NPs of CYP exhibited sustained release properties along with their comparable therapeutic potential with lower doses.
2	(Alhakamy & Md, 2019)	Repurposing Itraconazole Loaded PLGA Nanoparticles for Improved Antitumor Efficacy in Non-Small Cell Lung Cancers	Chitosan-coated PLGA nanoparticles of itraconazole	Single emulsion-sonication	ITR NPS of acceptable particle size were successfully formed, which showed higher cytotoxic, and apoptotic cell death

					in the H1299 cell line.
3	(Solanki, et al., 2015)	FORMULATION AND EVALUATION OF CYCLOPHOSPHAMIDE LOADED CHITOSAN NANOPARTICLES CONJUGATED WITH FOLIC ACID FOR CANCER TARGETING	Cyclophosphamide loaded folate-chitosan conjugated nanoparticles	Ionic cross linking technique	Folate coated CYP-CS-NPs were able to attach to cancer cells easily, reduced the dose of drug required, minimized the adverse events and improved the effectiveness of drug.

3.0 Materials and Methods

3.1 Materials

Itraconazole was an offering from Metrochem API Private Limited (Batch No. ITC/2101021) while Cyclophosphamide was procured from Lianyungang Guike Pharmaceutical Co., LTD (Batch No. 20230501). Chitosan was purchased via Sigma-Aldrich, Dichloromethane (procured from Duksan Pure Chemicals), Phosphate buffer Saline (PBS) (BR0014G), Dimethyl_sulphoxide (Procured from reagents, DAEJUNG), Dialysis tubing (14.3mm, MWCO 12,000-14,000 Daltons) was procured from Medicell Membranes Ltd. Breast Cancer Cell Lines were provided by Dr. Nadeem from Centre of Excellence in Molecular Biology (CEMB). All other reagents and solvents were of appropriate standards requiring no further purification.

3.2 Methods

3.2.1 Preparation of Cyclophosphamide Loaded Chitosan Nanoparticles

CYP-CS-NPs were created using the Ionic Cross-Linking Technique. To do this, 100 mg of Chitosan was dissolved in 10 ml of 1% glacial acetic acid and stirred continuously at a constant speed of 200-300 rpm for 60 minutes. It was then kept overnight at room temperature to get a clear Chitosan gel solution. pH was adjusted to 5. 10ml of TPP solution (1%) was added drop wise to the CS-Gel solution containing 100mg cyclophosphamide under continuous stirring for 40-60 mins at constant speed of 200-300 rpm. The resultant nanoparticle suspension was left overnight followed by the centrifugation the next day, at 12,000 rpm for 60 mins. After the particles settled, a clear supernatant solution appeared. The particles obtained from centrifugation were then freeze-dried and stored in an airtight container. The particle formation resulted from the interaction between the negatively charged groups of TPP and the positively charged amino groups of chitosan, a process known as ionic gelation

3.2.2 Preparation of Itraconazole Loaded Chitosan Nanoparticles

ITZ-CS-NPs were also prepared by Ionic Gelation method. 100mg of Chitosan was mixed and dissolved in 10ml 1% of Glacial acetic acid and stirred continuously for 60 mins at constant speed of 200-300 pm. Itraconazole 1% solution (100mg ITZ in DMSO) was added in CS Gel Solution with constant stirring; polymer drug ratio 1:2. 10ml TPP Solution (50mg TPP in 10ml DW) was added dropwise to ITZ-CS Solution at
constant rate of 0.5ml/min under constant stirring for 40-60 mins at 200-300rpm. Above solution was sonicated at frequency of 10,000 MHz for 15 minutes. After this step, solution was subjected to centrifugation at 12,000 rpm for 60 minutes. Small pellets were formed, which were washed with ultra-pure water and were lyophilized for further characterization.

3.2.3 Percent Encapsulation Efficiency (EE)

After the formulation of NPs, the supernatant which was previously collected after the centrifugation, was assessed with the total quantity

of drug initially used to determine the efficiency of dug loading of the NPs. Amount of unentrapped drug dispersed in the supernatant
was measured using UV-visible spectrophotometry (cuvette type), (SHIMADZU, Model: UV-1800 240V, JAPAN) at the detection wavelength λ-max of 262 nm. The indirect % EE of drug encapsulated in the NPs (EE) was evaluated by using the formula as given:

$$EE = \frac{\text{(Total mass of drug in NPs)} \times \text{(Calculated amoun of free drug in supernatant)}}{Total\ mass\ of\ drug\ used\ (mg)} \times 100 \ldots\ldots (3.1)$$

3.2.4 Drug Loading Capacity

Drug content analysis was carried out to quantify the drug loading in the Chitosan based nanoparticles by comparing with standard drugs; CYP and ITZ. This study was conducted using UV spectrophotometer and absorbance was measured at λ-max of both drugs (262nm). The percentage of CYP & ITZ loaded in the NPs; drug loading (DL) was evaluated by applying the following formula:

$$DL \quad \frac{\text{(Quantity of drug in NPs)} \times \text{(Weight of NPs)}}{\text{Total amount of drug used (mg)}} \times 100b \ldots. (3.2)$$

3.3 Characterization

3.3.1 Fourier Transform Infrared Spectroscopy (FTIR)

Spectra using Fourier transform infrared spectroscopy were obtained for Chitosan polymer, Chitosan nanoparticles, ITZ, CYP, and ITZ-CS-NPs and CYP-CS-NPs via ALPHA FTIR Spectrometer from BRUKER, United States). The samples were prepared in KBr disks in the IR region of 4000–400 cm^{-1}. Three scans in total were obtained for each sample and the best one chosen for comparison.

3.3.2 Particle Size Analysis

Analysis of Particle Morphology and its size, polydispersity index (PDI) and zeta potential of ITZ-CS-NPs, CYP-CS-NPs and CS-NPs were determined by using Zetasizer analyzer. For proper analysis, NPs samples were properly diluted with deionized water to 10 times of their volume and then they were sonicated for 30 minutes to diminish particle adhesion. Using Broakhaven software, the measurement parameters (wavelength (1000 nm), viscosity (0.8872 cP), and refractive index (1.33) were adjusted (Saed Aldalaen et al., 2019).

3.3.3 SEM-EDX

The surface morphology of ITZ-CS-NPs, CYP-CS-NPs and CS-NPs was observed via SEM, which was performed using the Nova Nano-SEM 450 field-emission scanning electron microscope (FE-SEM). The samples were coated with gold under vacuum before imaging. Micro-images were obtained in different resolutions ranging from 50 – 300μm.

3.4 In Vitro Drug Release

Based on Concerned Literature, a common method knows as dialysis membrane method was employed to establish in vitro drug release of ITZ & CYP from the CS nanoparticles. Dialysis membrane bags were soaked overnight in release media (Phosphate Buffer Saline, PBS) pH 7.4 prior to in vitro release experiment. In brief, dispersion of 50 mg of ITZ-CS-NPs and CYP-CS-NPs in 2mL was carried out PBS (pH 7.4) containing 5% (v/v) tween 80 separately and this suspension were taken into dialysis bags (12,000-14,000 molecular weight), that should be tightly sealed to avoid the leakage. Using 100ml beaker, this dialysis bag was dipped in the 30 mL solution of PBS consisting of 5% (v/v) tween 80, with stirring maintained at 100 rpm and 37°C to ensure the sink conditions for CYP and ITR. At fixed intervals (0.25, 0.5, 1, 2, 4, 6, 8, 12, 24, 48 hours), the 2mL sample drawn and were substituted with fresh 2mL fresh PBS containing 5% (v/v) tween 80 each time (Saed Aldalaen et al., 2019). The concentration of the free ITZ and CYP in the samples withdrawn from PBS was calculated by UV at 262 nm (wavelength of maximum absorption). Later, the accumulative ratios of the released ITZ and CYP were measured as a function of time. All measurements were

carried out three times (Hamidreza Kheiri et al., 2019). The cumulative drug release measurements were plotted over a 48-hour period.

3.5 Cytotoxic Assay

The cytotoxic-effects of the free Itraconazole (ITZ), cyclophosphamide (CYP), ITZ-CS-NPs and CYP-CS-NPs on the HepG2 and MCF-7 are studied by using MTT (3- [4, 5- dimethylthiazol-2yl]-2, 5-diphenyl tetrazolium bromide) assay. Briefly, 2×96 HepG2 and MCF7 cells/well are seeded into 96-well plates (flat bottom) and incubated at a temperature of 37°C, CO2 concentration of 5%, for 24 hours to allow the cells to attach. Next day, after reaching up to 70% confluency, the cells are treated with the various concentration of free, and as well encapsulated forms of ITZ and CYP (10-300µg/ml) and then incubated at the temperature of 37°C, CO2 concentration of 5%, and 95% relative humidity for 24 hours. Cells without the test samples (drugs.) are used as controls and each tests sample, and control are tested in triplicates. After the incubation against indicated time period (24 hours), 20µl of MTT reagent (5mg/ml in DMSO) are added in the each well and then incubated again for 4 hours. After this, 80% of medium with MTT are pipetted out, and the formazan-crystals formed are solubilized in the 150µl of DMSO. The numbers of the living cells after the particular treatment are counted by the measuring absorbance of formazan at wavelength 570nm in the ELISA-plate-reader (RT-6000, Rayto, Germany) with the reference wavelength 630 nm. All of these experiments are done in triplicates.

4.0 Results

In the present study, Cyclophosphamide and Itraconazole loaded nanoparticles were prepared using the biodegradable polymer Chitosan (CS). The CYP-CS-NPs & ITR-CS-NPs were prepared using the Ionic Gelation method and characterized by various techniques to determine the physiochemical properties. The cytotoxic assay of the polymeric nanoparticles was performed to investigate the anti-cancer properties of nanoparticles against Beast carcinoma cells (MCF-7 cells).

4.1 Percentage Entrapment Efficiency (EE)

The percentage entrapment efficiency of prepared nanoparticles was determined by using equation 3.1. Percentage Entrapment efficiency of CYP-CS-NPs & ITR-CS-NPs was measured after taking the mean of 3 preparations.

Table 4.1: Evaluation of drug loaded CS nanoparticles

Formulation	Particle Size	PDI	EE (%)	LC (%)
NP's Empty	335.9 nm	0.569	-	-
NP's + CYP	213.3nm	0.583	62.64	50
NP's + ITR	412nm	0.508	98.79	50

4.2 Drug Loading Capacity

The drug loading capacity of the prepared nanoparticles was calculated using equation 3.2 and is presented in table 4.1. Calibration curves for Cyclophosphamide and Itraconazole were used to determine the concentration of unknown samples, as shown in figures 4.1 and 4.2 for CYP, and figure 4.3 for ITR.

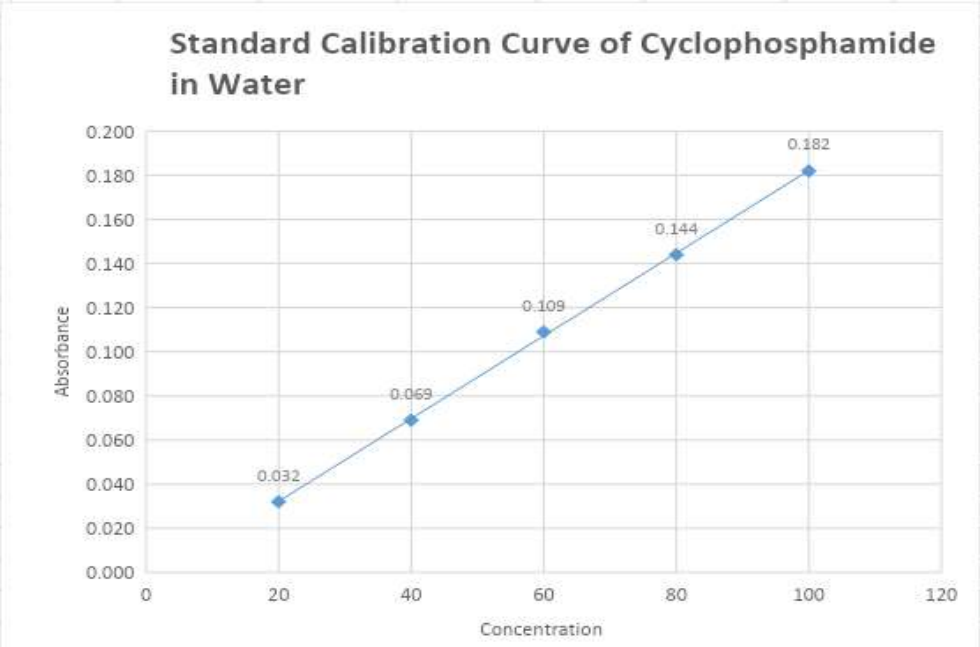

Figure 4.1: Calibration Curve of Cyclophosphamide in Water

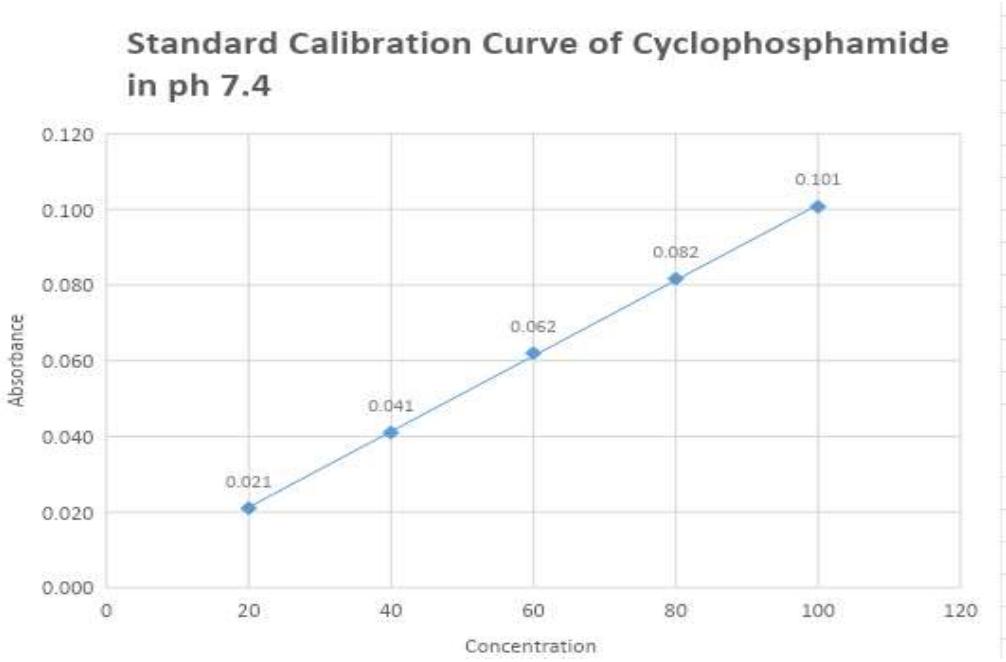

Figure 4.2: Calibration Curve of Cyclophosphamide in pH 7.4

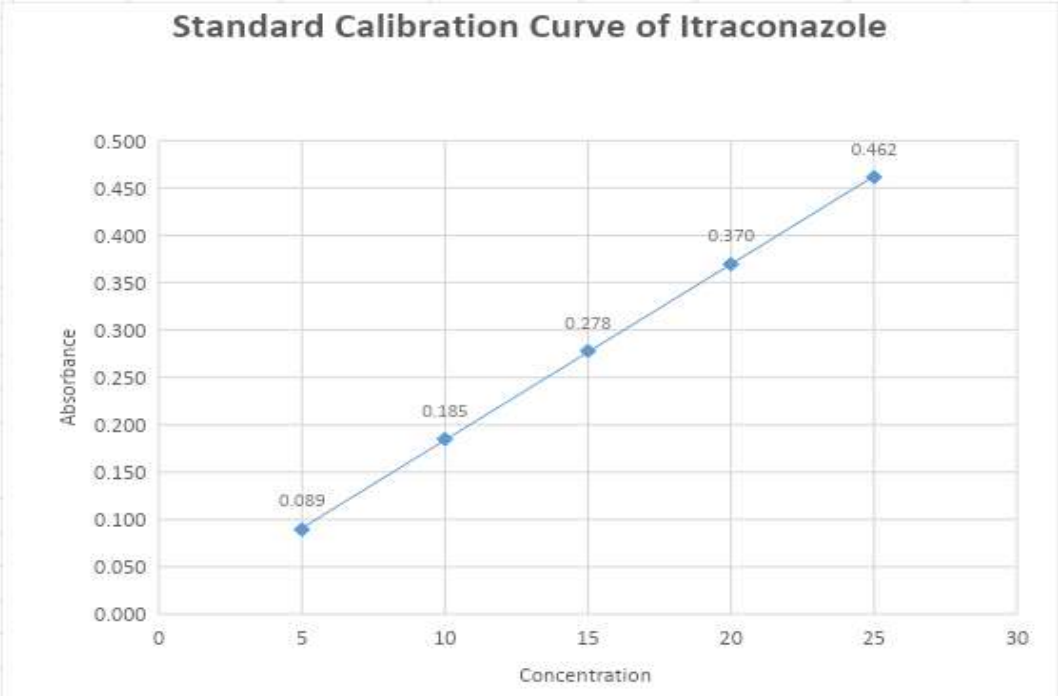

Figure 4.3: Calibration Curve of Itraconazole.

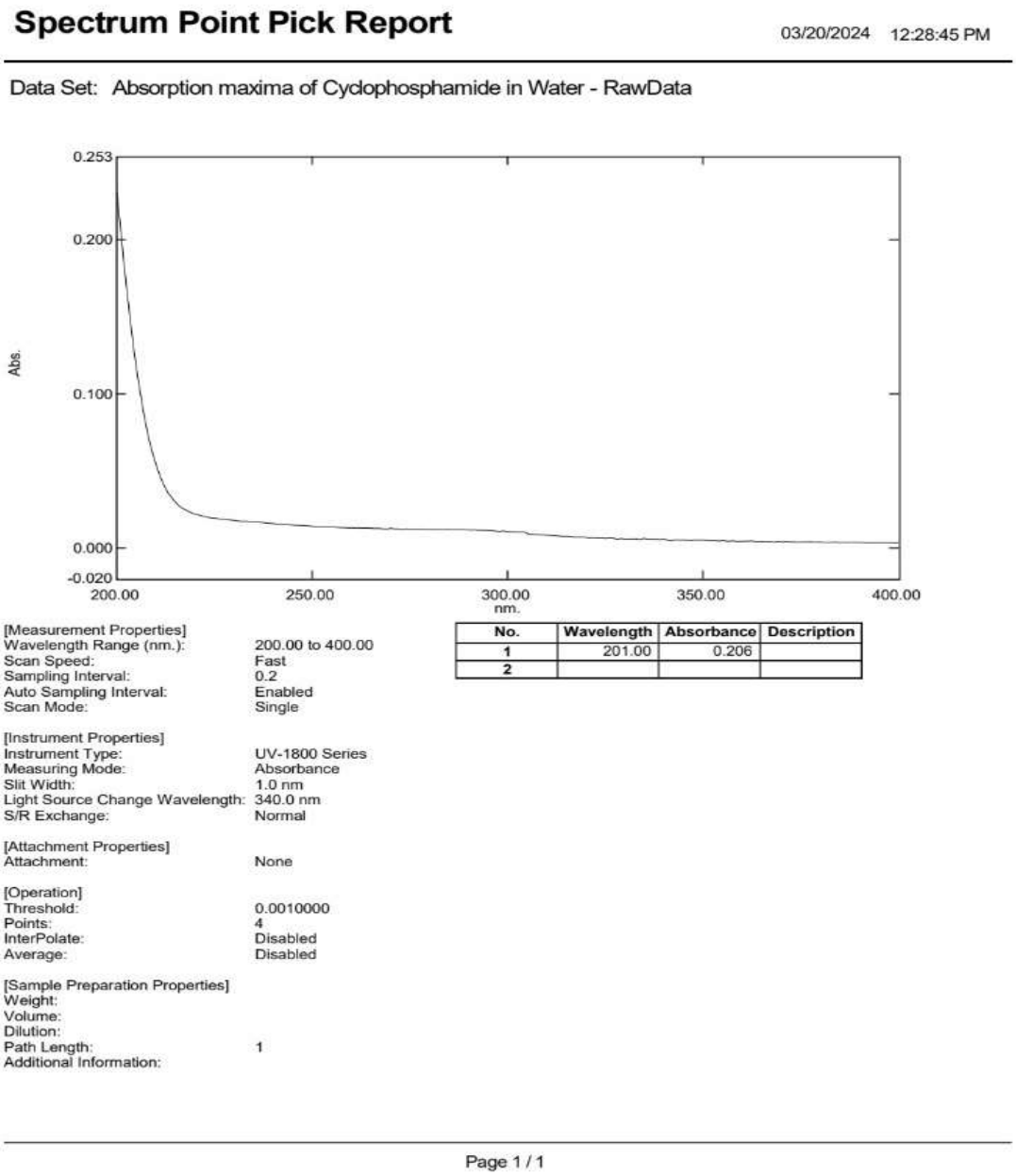

Figure 4.4: Absorption Maxima of Cyclophosphamide Nanoparticles

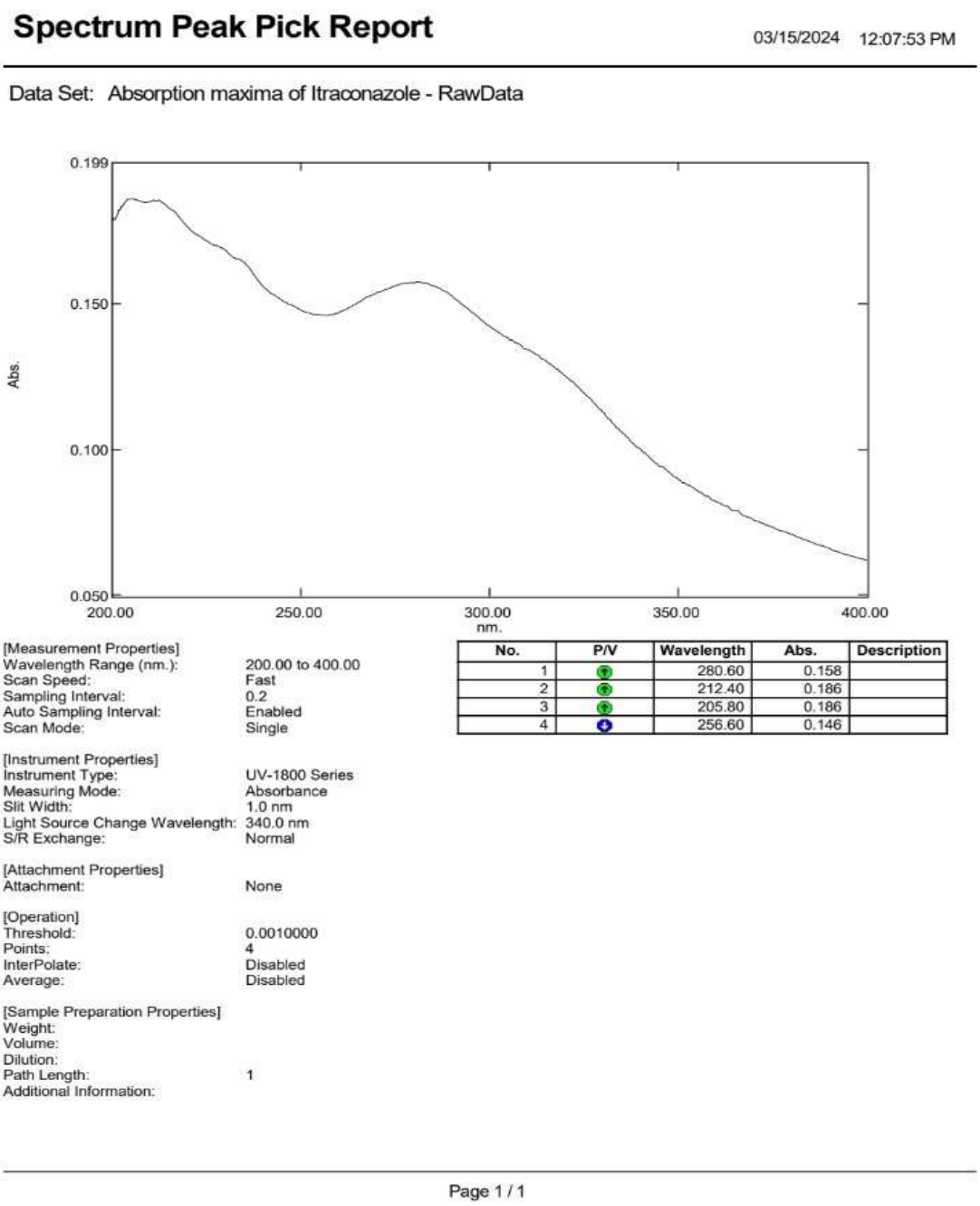

Figure 4.5: Absorption Maxima of Itraconazole Nanoparticles

4.3 FTIR

The prepared nanoparticles were subjected to Fourier transfer infrared analysis (FITR) to determine characteristic peaks of pure drug in final prepared nanoparticles with polymer. The spectra of pure Cyclophosphamide, pure Itraconazole, polymer and final formulations were recorded and compared with each other.

4.3.1 FTIR analysis of Cyclophosphamide loaded CS nanoparticles

The IR spectra of CYP show characteristic peaks at 3431, 2976, 1649, 1453, and 1090 cm^{-1}, which correspond to the phospho-ketone and phospho-carbonyl groups of CYP. The peak present at 1550 cm^{-1} is attributed to the N-H group's stretching bands, while the peak at 817 cm^{-1} is due to the C-O-P stretching bands. Additionally, the peaks at 878 cm^{-1} and 736 cm^{-1} appear because of the wagging and deformation of bonds in the secondary amine (NH), respectively.

The Chitosan Spectrum presents characteristic peak at 3322 cm^{-1} due to N-H and O-H stretching, as well as intermolecular Hydrogen bond, absorption peak at 2918 cm^{-1} and 2877 cm^{-1} for C-H both symmetric as well as asymmetric stretching respectively, at 1559 cm^{-1} associated with N-H bending. The residual N-acetyl groups were asserted by the bands around 1718 cm^{-1} (C=O stretching of amide I) and 1373 cm^{-1} (C-N stretching of amide III), respectively. The bands present at 1405 cm^{-1} and 1375 cm^{-1} corresponds to CH3 bending and CH3 deformation. The other characteristic bands of CS polymer, which showed C–O–C bridge, emerged at 1155 cm^{-1} and the bands at 1053 cm^{-1} and 1019 cm^{-1} represents C-O stretching.

It was observed that all the characteristic bands of CS and CYP are detectable in CYP-CS NPs IRs. Thus, it can be concluded with the loading and interaction of CYP into CS NPs.

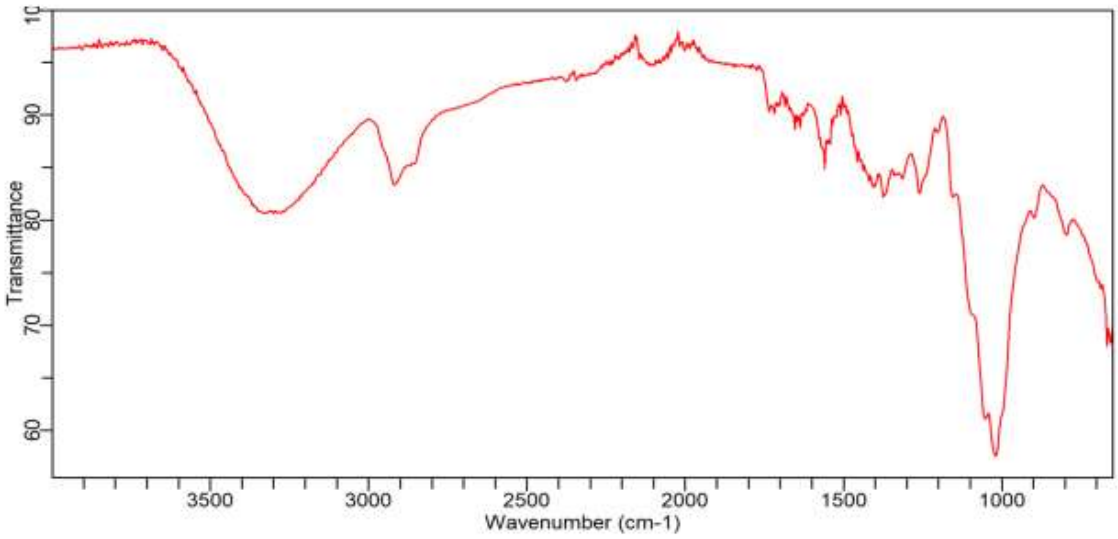

Figure 4.6: FTIR Spectra of Chitosan Blank NPs

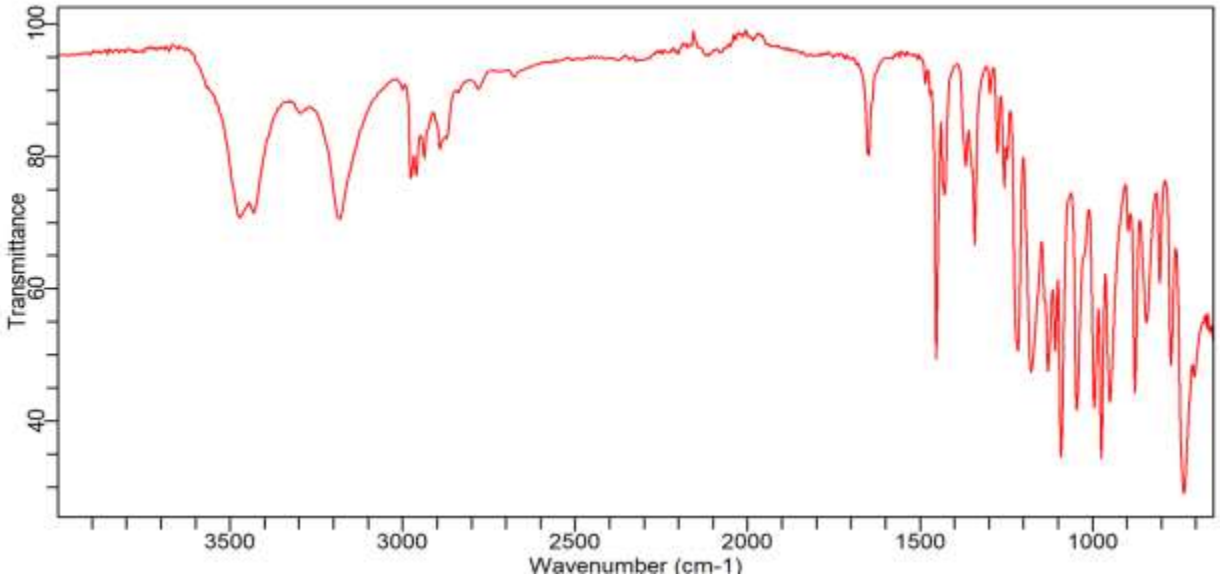

Figure 4.7: FTIR Spectra of Cyclophosphamide

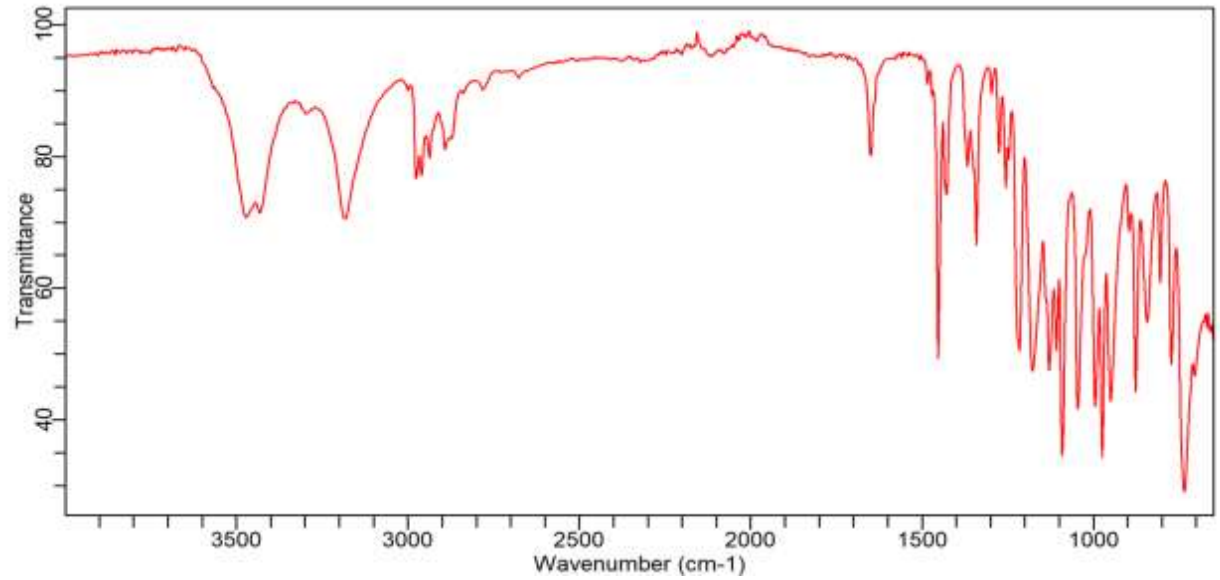

Figure 4.8: FTIR Spectra of CYP-CS Nanoparticles.

Table 4.2: Major bands of FTIR of Cyclophosphamide, Chitosan and CYP-CS NPs

Bands	Wavenumber (cm^{-1})			
	Cyclophosphamide	Chitosan	CYP-CS NPs	Functional Group
1	-	3322	3235	OH Stretching
2	-	2918	-	symmetric stretching of C-H
3	-	2877	-	asymmetric stretching C-H
4	-	1718	-	C=O stretching of amide

5	-	1559	-	N-H Bending
6	1550		1533	N-H Stretching
7	1453	1405	1457	CH3 bending
			1420	
8	-	1375	1379	CH3 deformation
9	-	1373	1325	C-N stretching
10	-	1155	-	C–O–C bridge
11	1090	1053	1067	C-O stretching
		1019	1019	
12	817	-		C-O-P Stretching
13	878	-		NH wagging
14	736	-		NH deformation
15	974	-	948	C-H Bending

4.3.2 FTIR analysis of Itraconazole loaded CS nanoparticles

The spectra revealed characteristic peaks for itraconazole at 2951, 2931, 2875, 2821, 1695, 1507, 1450, and 670 cm^{-1}. The absorption bands between 2800 and 3200 cm^{-1} were attributed to alkane, aromatic CH, and amine groups. Peaks at 1507 and 1217 cm^{-1} correspond to C=N and C-N bonds, respectively, while the sharp peak at 1695 cm^{-1} is due to the C=O bond of the drug. The IR region from 1400 to 600 cm^{-1}, known as the fingerprint region, contains many unassigned vibrations. Additionally, the FTIR spectrum of itraconazole-loaded nanoparticles with chitosan showed fewer characteristic peaks of itraconazole, indicating successful loading of ITR into CS NPs..

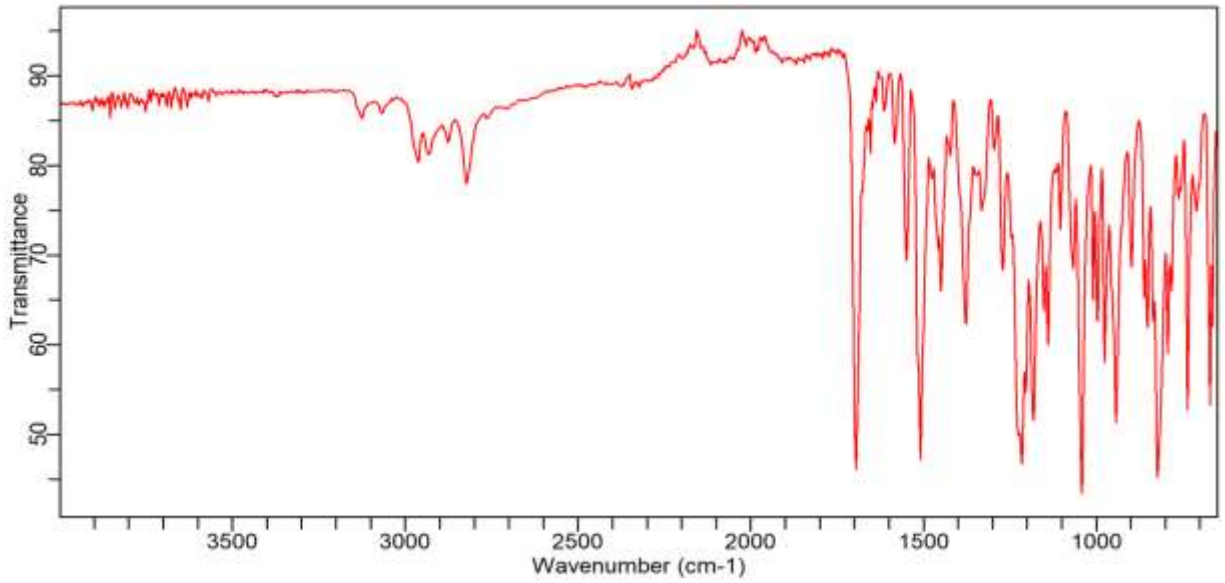

Figure 4.9: FTIR Spectra of Itraconazole

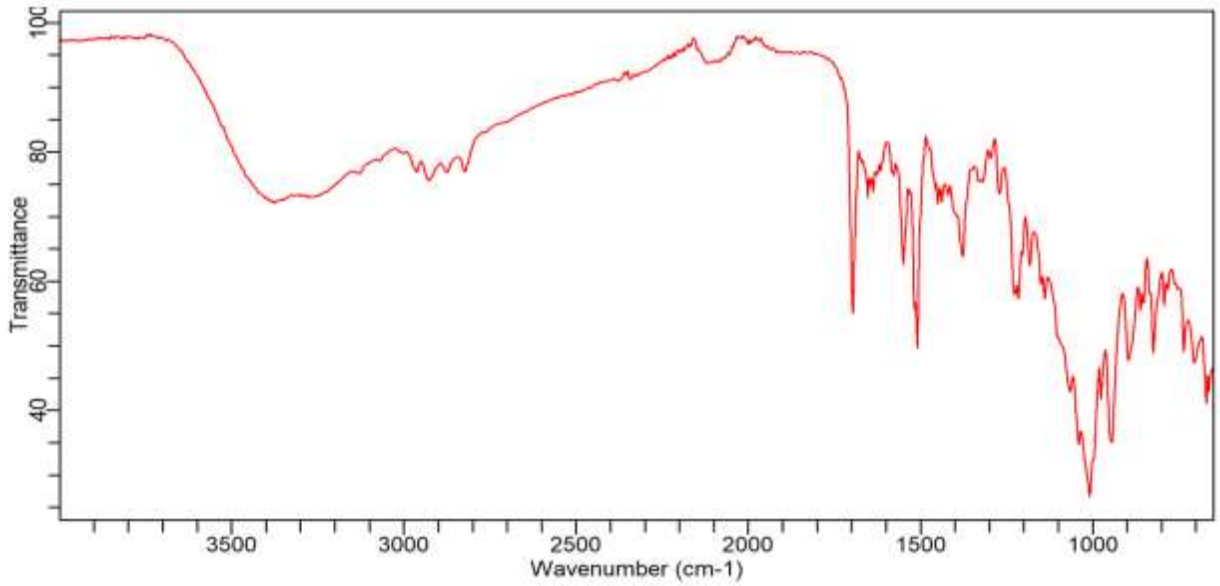

Figure 4.10: FTIR Spectra of ITR-CS Nanoparticles

Table 4.3: Major bands of FTIR of Itraconazole, Chitosan and ITR-CS NPs

Bands	Wavenumber (cm^{-1})			
	Itraconazole	Chitosan	ITR-CS NPs	Functional Group
1	-	3322	3375	OH Stretching
2	2961	2918	2961	C-H symmetric stretching
	2931		2927	
3	2875	2877	2875	C-H asymmetric stretching
	2821		2823	
4	-	1718	-	C=O stretching of amide
5	1695		1697	C=O
6	-	1559	-	N-H Bending
7	1507		1507	C=N
8	1401	1405	1457	CH3 bending
			1420	
9	-	1375	1379	CH3 deformation
10	-	1373	1325	C-N stretching of amide III
11	1217	-	-	C-N bond
12	-	1155	-	C–O–C bridge
13	1041	1053	1041	C-O stretching
		1019	1008	

4.4 Particle Size Analysis

Size of CS based Cyclophosphamide and Itraconazole nanoparticles was determined with the help of Malvern mastersizer instrument.

4.4.1 Particle size of Cyclophosphamide loaded CS nanoparticles

Analysis of particle size demonstrated a coherent disposition of all the particles, average size of which were 335.9 nm and a polydispersity index of 0.569 for CS-NPs. In case of CYP-CS-NPs, they presented an average diameter of 213.3 nm and a polydispersity index of 0.583. It could be said from this data, that the successfully formed nanoparticles are capable to pass through biological barriers with improved drug delivery due to their small size, which in turn enhances efficiency.

4.4.2 Particle size of Itraconazole loaded CS nanoparticles

The average diameter of ITR-CS-NPs came out to be 412.1 nm and poly-dispersity index was 0.508. The average of size and poly-dispersity index of CS-NPs is 335.0 and 0.569 respectively, it can be said that the ITR-CS-NPs have also been made successfully.

4.5 SEM

Scanning electron microscopy (SEM) was again undertaken to constitute the morphology of chitosan based Cycophosphamide and Itraconazole nanoparticles.

4.5.1 SEM Analysis of Cyclophosphamide Loaded-Chitosan Nanoparticles

The formulation was characterized for its morphology and shape by SEM under various magnifications.

The figure 4.11, 4.12 and 4.13 revealed very homogenous morphology.

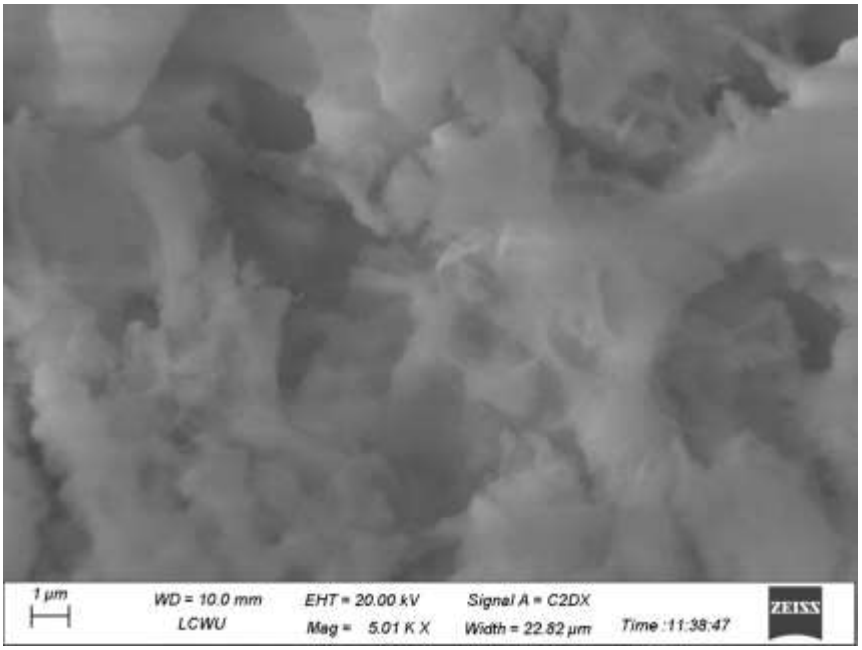

Figure 4.11: SEM images of CYP-CS Nanoparticles (22.82 µm)

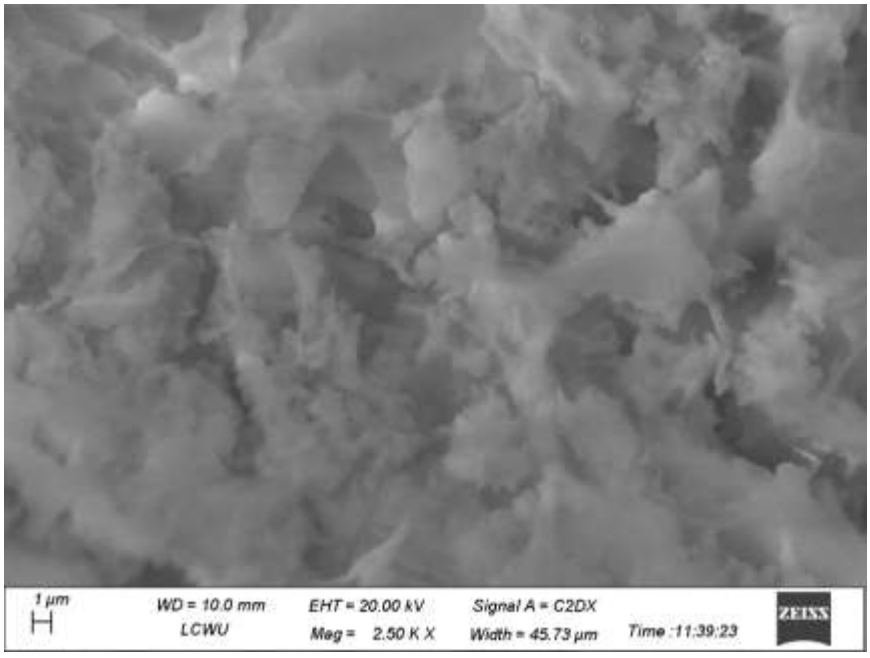

Figure 4.12: SEM images of CYP-CS Nanoparticles (45.73 µm)

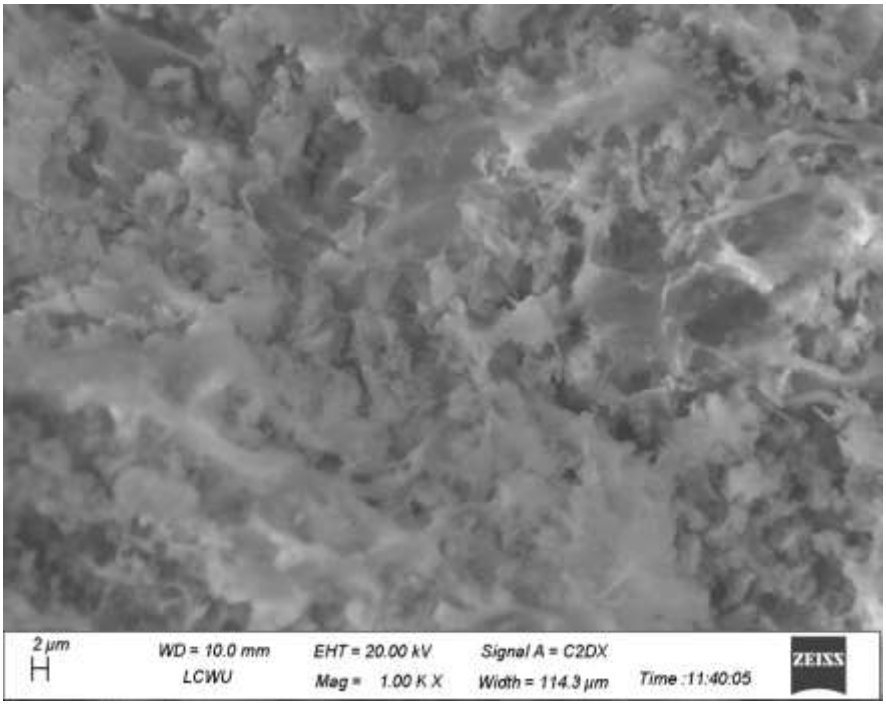

Figure 4.13: SEM images of CYP-CS Nanoparticles (114.3µm)

4.5.2 SEM Analysis of Itraconazole Loaded-Chitosan Nanoparticles

When observed under the microscope, figure shows that the nanoparticles had a smooth globular surface as shown in figure 4.14 and 4.15. Agglomeration can also be seen in figure shown below.

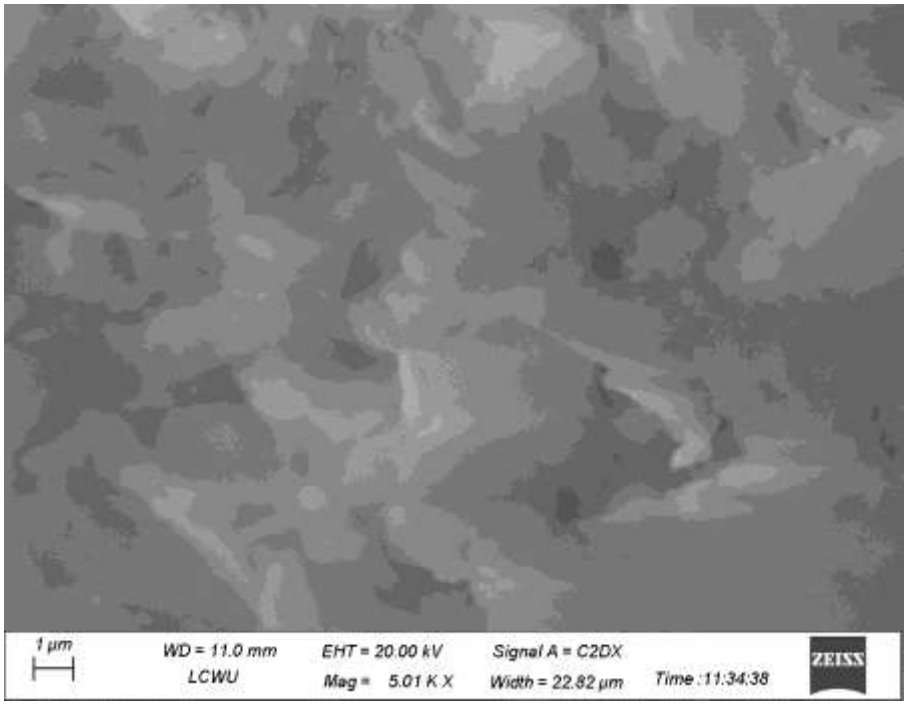

Figure 4.14: SEM images of ITR-CS Nanoparticles (22.82µm)

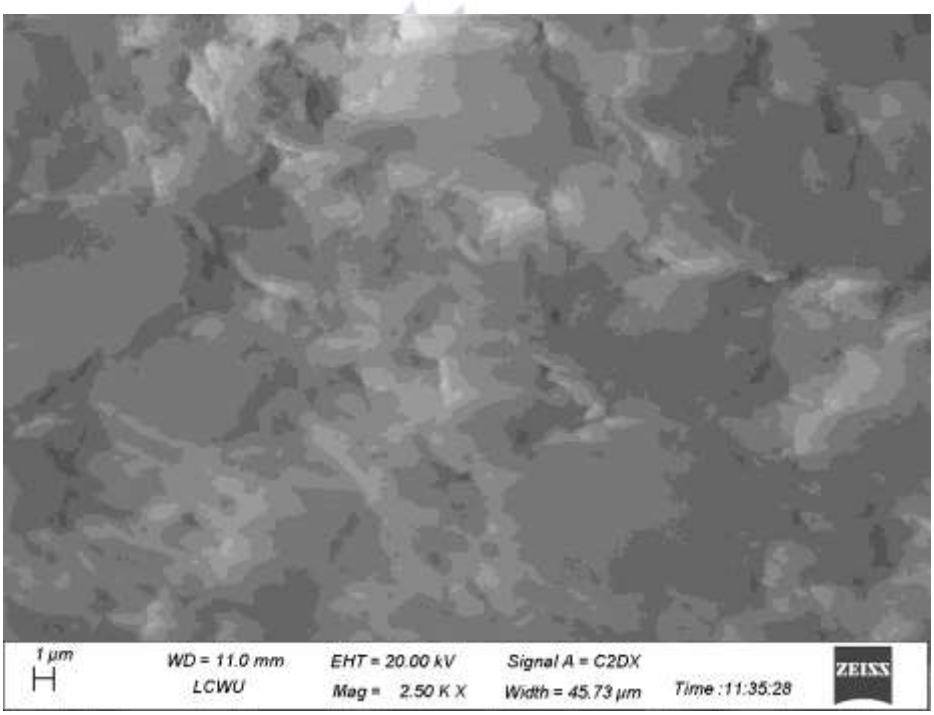

Figure 4.15: SEM images of ITR-CS Nanoparticles (45.73 µm)

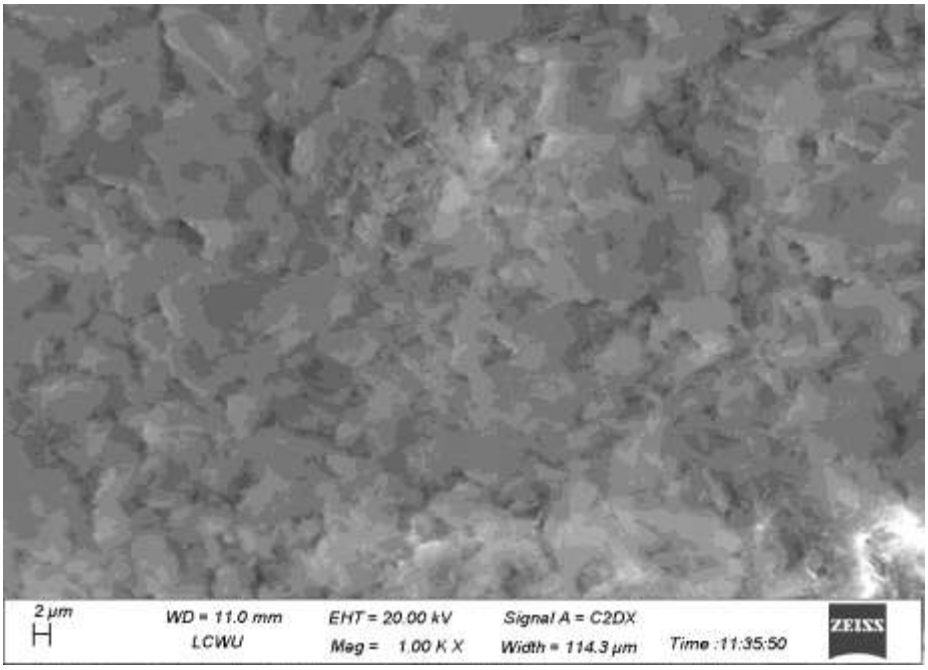

Figure 4.16: SEM images of ITR-CS Nanoparticles (114.3 µm)

4.6 In-Vitro Release Profile

The dialysis membrane method was used to assess the in-vitro release of CYP-CS-NPs & ITR-CS-NPs at a pH of 7.4.

4.6.1 In-Vitro Release Profile of Cyclophosphamide Loaded-Chitosan Nanoparticles

The formulation exhibited a biphasic release pattern, with an initial burst release of the drug at 6 hours, followed by a sustained release of Cyclophosphamide over 48 hours. The results are detailed in Table 4.4 and illustrated in Figure 4.17.

Table 4.4 In-vitro release profile of CYP-CS-NPs

Sr. No.	Time (hours)	Absorbance at 264nm	Concentration of drug release calculated from slope (mg/ml)	Amount of drug in mg	% Drug Release
1	0	0	0	0	0
2	0.5	0.391	0.22904	0.309206021	7.730151
3	1	0.421	0.55871	0.754260966	18.85652
4	2	0.445	0.82244	1.110304922	27.75762
5	4	0.471	1.10816	1.496019207	37.40048

6	6	0.493	1.34992	1.822392834	45.55982
7	8	0.509	1.52574	2.059755471	51.49389
8	24	0.555	2.03123	2.742173054	68.55433
9	48	0.581	2.31695	3.127887339	77.8263

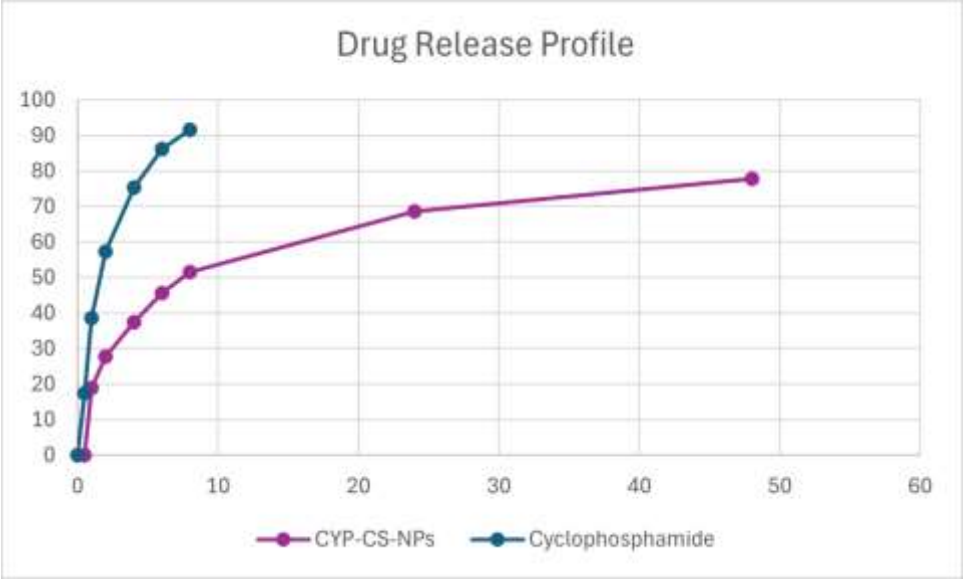

Figure: 4.17 In-vitro release profile of CYP-CS-NPs

4.6.1 In-Vitro Release Profile of Itraconazole Loaded-Chitosan Nanoparticles

The formulation showed a steady release throughout the time period of 48 hours. Results are shown in table 4.5 along with the graph as in figure 4.18.

Table 4.5 In-vitro release profile of ITR-CS-NPs

Sr. No.	Time (hours)	Absorbance at 264nm	Concentration of drug release calculated from slope (mg/ml)	Amount of drug in mg	% Drug Release
1	0	0	0	0	0
2	0.5	0.395	0.238692	0.322234	8.055852
3	1	0.404	0.337593	0.455751	11.39376
4	2	0.42	0.513417	0.693113	17.32783
5	4	0.449	0.832098	1.123333	28.08332

6	6	0.481	1.183747	1.598058	39.95146
7	8	0.505	1.447483	1.954102	48.85256
8	24	0.549	1.931	2.606849	65.17124
9	48	0.569	2.15078	2.903553	72.58882

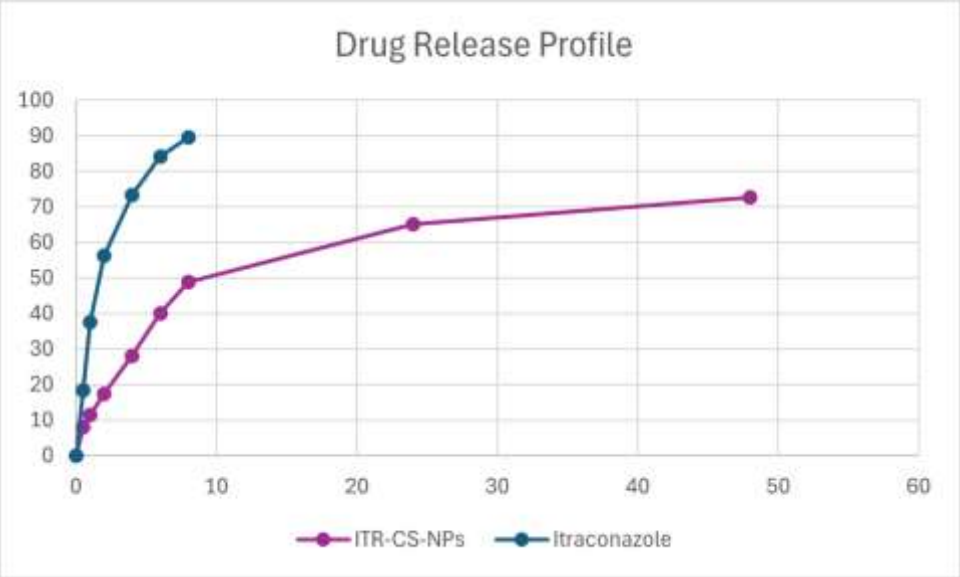

Figure: 4.18 In-vitro release profile of ITR-CS-NPs

4.7 Cytotoxic Assay

In this study, the cytotoxic effects of free CYP, ITR, different concentrations of CYP-CS-NPs and ITR-CS-NPs on MCF-7 cancer cells after 24 hours of incubation were assessed using colorimetric MTT assay.

4.7.1 Cytotoxic Assay of Cyclophosphamide Loaded-Chitosan Nanoparticles

The MTT assay results of cytotoxic activity of CYP and CYP-CS-NPs against MCF-7 cells are shown in figure 4.19.

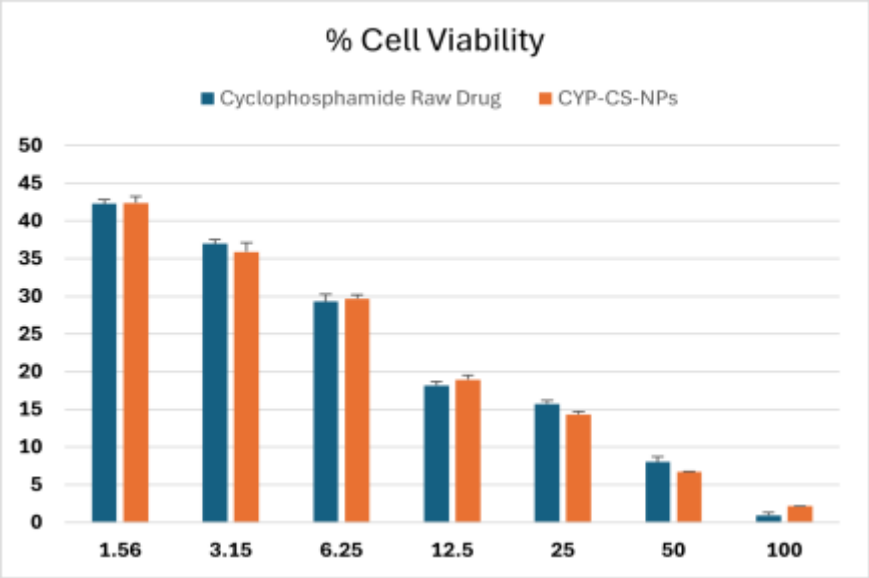

Figure 4.19: MTT assay for cell viability of MCF cells (CYP and CYP-CS-NP)

According to the MTT assay, the cytotoxicity of Cyclophosphamide nano formulations were comparable to pure Cyclophosphamide. The cytotoxic effect on MCF-7 cells was dose-dependent exhibiting the sustained cytotoxic effect.

4.7.2 Cytotoxic Assay of Itraconazole Loaded-Chitosan Nanoparticles

The MTT assay results of cytotoxic activity of ITR and ITR-CS-NPs against MCF-7 cells are shown in figure 4.20.

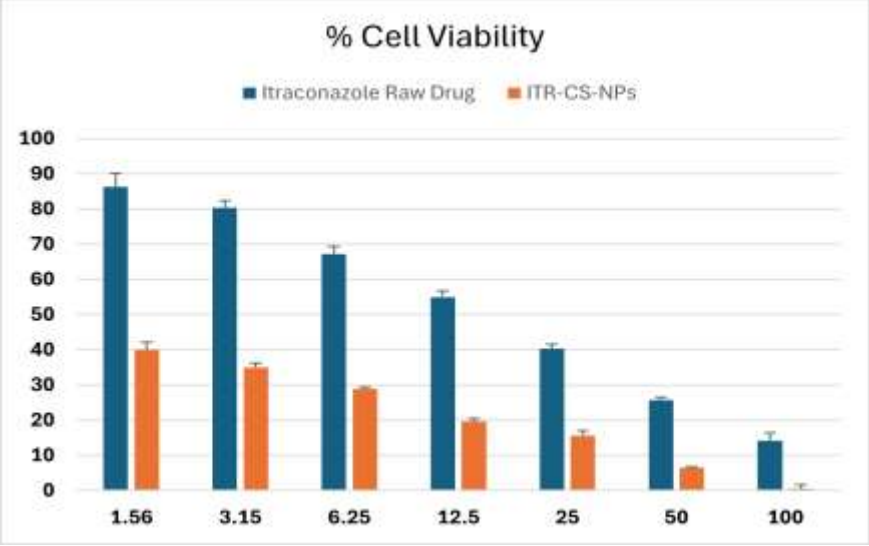

Figure 4.20: MTT assay for cell viability of MCF cells (ITR and ITR-CS-NP)

According to the MTT assay, Itraconazole nano formulations were less cytotoxic than pure Itraconazole. The cytotoxic effect on MCF-7 cells was dose-dependent, with Chitosan nanoparticles loaded with Itraconazole exhibiting the sustained cytotoxic effect.

5. Discussion

Cyclophosphamide is a chemotherapeutic agent that suppresses the immune system and is primarily used for the treatment and management of neoplasms, including breast cancer, multiple myeloma, and sarcoma (Ogino & Tadi, 2023). It

was considered to be the most effective anti-cancer molecule ever (Eslam Dabbish, 2023). It was first approved in 1959 as the eighth cytotoxic agent for the treatment of cancer.

Cyclophosphamide has also been extensively used as an immunosuppressant in lupus-related systemic erythema, bone marrow transplant immunoablations, rheumatoid arthritis, and other autoimmune inflammatory conditions. It treats a variety of solid, hematologic, and childhood cancers, such as Hodgkin's lymphoma, multiple myeloma, chronic myeloid leukemia, small cell lung cancer, uterine cancer, Burkitt's lymphoma, multiple sclerosis, neuroblastoma, endometrial cancer, and renal disorders unresponsive to corticosteroids. (Eslam Dabbish, 2023).

Cyclophosphamide exerts anti-cancer effects by cross-linking DNA strands, inhibiting cell division, and stimulating apoptosis in rapidly dividing cells (Jiang M, 2020). However, it can also induce cytotoxic effects on normal cells, which are dose-dependent. These effects, including bone marrow suppression, cardiac and gonadal toxicity, hemorrhagic cystitis, and carcinogenesis, are linked to its metabolism and inactivation by aldehyde dehydrogenase, with cumulative dose being the main risk factor. (Ashkan Emadi, 2009)Advanced drug delivery systems, particularly nanoparticle-based therapies, have been explored to reduce these toxic effects and overcome multidrug resistance. (Shreelaxmi Gavas, 2021)

Itraconazole, an FDA-approved antifungal, is the second drug used in this study. This research repurposes itraconazole as an anti-cancer agent, as screening studies have shown its anti-cancer activity via inhibition of the hedgehog pathway (Chun-Lan, et al., 2022).

Drug repurposing provides a solution to the challenges of developing novel anti-cancer drugs, which include high costs, long development times, regulatory hurdles, and high failure rates. Itraconazole has multiple molecular targets, reducing the likelihood of resistance while being effective against various malignancies, demonstrating its potential as a novel anti-tumor agent. (Chun-Lan, et al., 2022) In this study, polymer-based cyclophosphamide and itraconazole nanoparticles were synthesized using chitosan as the polymer, characterized, and tested for anti-cancer potential against MCF-7 cell lines. The use of biodegradable polymers addresses the limitations of non-biodegradable polymers, with chitosan being biocompatible, biodegradable, and muco-adhesive, making it suitable for drug-loaded nanoformulations. Chitosan is one of the biodegradable polymers that are most frequently manufactured (CS) because of its complete biodegradability and biocompatibility, controlled characteristics, simple processing, and well-defined formulation procedures. CYP-CS-NPs and ITR-CS-NPs were prepared by ionic crosslinking method/ionic gelation method followed by freeze drying. There were no publications following the same method using chitosan as polymer. Characterization of CYP-CS-NPs and ITR-CS-NPs was performed. According to Table 4.1, the CYP-CS nanoparticles showed 62.64% entrapment efficiency (EE), while ITR-CS nanoparticles displayed 98.79% EE. The CYP-CS NP size and poly-dispersity index (PDI) were 213 nm and 0.583, respectively, while ITR-CS NPs had particle size 412 nm and PDI 0.508. This demonstrates that both cyclophosphamide and itraconazole were encapsulated successfully. Particle size measurements (Table 4.1) indicate that ITR-CS NPs were larger than blank CS NPs, showing that the volume of NPs increased with drug incorporation; however, CYP-CS-NPs were smaller than CS NPs, indicating easier penetration at the target site. The polydispersity index reflects the distribution of polymeric chain molecular weights. The prepared polymeric nanoparticles had a PDI value of less than 0.6, indicating slightly tight constrained polymer distribution and a monodisperse system.

FTIR analysis confirmed successful formation of CYP-CS and ITR-CS nanoparticles, with characteristic peaks of drugs and chitosan observed (Figs. 4.6–4.10). Figure 4.8 demonstrated the characteristic peaks of both CYP and CS, confirming successful nanoparticle formation. The FTIR spectrum of itraconazole-loaded nanoparticles containing chitosan showed very few characteristic peaks of itraconazole, indicating successful loading into CS NPs. SEM analysis determined the morphology and nature of the

nanoparticles. Cyclophosphamide CS nanoparticles had a smooth circular surface with minor aggregation, while itraconazole CS nanoparticles showed a globular surface with **agglomeration (Figs. 4.11–4.16).** Table 4.4 displays the release pattern for CYP studied using the dialysis method at pH 7.4. A burst release occurred in the first six hours, followed by sustained release over the next two days. For ITR-CS NPs, in-vitro release profiles showed continuous release from the polymeric phase over two days. The effects of CYP and ITR, along with their nanoparticles, were studied on MCF-7 cell lines to examine anti-cancer and apoptotic properties. IC50 was determined, and cell viability and cytotoxic limits were observed. The cytotoxic potential of ITR was noticeably enhanced in the NP formulation.

5.2 Study Limitations

Our research has certain limitations when it comes to using MCF-7 cell lines as an in-vitro Breast cancer study model. MCF7 is a valuable tool to study ontogenesis however, the breast cancer patient's population is quite diverse which makes the number of cell lines limited. Designing a study solely based on cell models is not enough. It is important to compare the findings from Cell study with those conducted on animal models. Also, it is difficult to obtain the clinical samples which are relevant to laboratory studies.

6.0 Conclusion

In this study, Polymeric Chitosan nanoparticles loaded with CYP and ITR were effectively synthesized separately using the ionic-gelation method. From pharmaceutical perspective, both CYP and ITR NPs with desirable properties particle size, morphological analysis, drug loading capacity and release were easily prepared and revealed that both CYP-CS-NPs and ITR-CS NPs exhibited spherical shapes with smooth surfaces. The synthesized nanoparticles demonstrated a prolonged release profile and good encapsulation effectiveness for 48 hrs indicating that they are well suited for this function. The MTT assay showed that at the doses used in the study, the cytotoxic effects of ITR-CS NPs were significant against MCF-7 cell lines. These results indicate that an attractive drug delivery strategy by encapsulating ITR in CS polymer in the form of nanoparticles in combination with CYP-CS NPs yet require further studies to estimate the cytotoxic potential of CYP-CS-NPs and ITR-CS-NPs on other cancer cell lines. The therapeutic efficacy of these nanoparticles needs to be further clarified by in vivo testing.

REFERENCES

Abotaleb, M., Kubatka, P., Caprnda, M., Varghese, E., Zolakova, B., Zubor, P., . . . Büsselberg, D. (2018, May). Chemotherapeutic agents for the treatment of metastatic breast cancer: An update. *Elsevier, 101*, 458-477. doi:https://doi.org/10.1016/j.biopha.2018.02.108

Alhakamy, N. A., & Md, S. (2019). Repurposing Itraconazole Loaded PLGA Nanoparticles for Improved Antitumor Efficacy in Non-Small Cell Lung Cancers. *Pharmaceutics, 11*(12), 685. doi:10.3390/pharmaceutics11120685

Ali MM, K. M. (2020). Primary care physicians and cancer care in Pakistan: a short narrative. *J Cancer Policy*. doi:25:100238. 10.1016/j.jcpo.2020.100238

Ashkan Emadi, R. J. (2009). Cyclophosphamide and cancer: golden anniversary. Retrieved from https://www.nature.com/articles/nrclinonc.2009.146

Bahreyni, A., Mohamud, Y., & Luo, H. (2020). Emerging nanomedicines for effective breast cancer immunotherapy. *Journal of Nanobiotechnology*. Retrieved from https://jnanobiotechnology.biomedcentral.com/articles/10.1186/s12951-020-00741-z

Barba, D., León-Sosa, A., Lugo, P., Suquillo, D., Torres, F., Surre, F., . . . Caicedo, A. (2023). Breast cancer, screening and diagnostic tools: All you need to know. *Elsevier.*

doi:https://doi.org/10.1016/j.critrevonc.2020.103174

Bhowmik, A., Laha, D., & Das, H. (2007). GrupSM Current Advances in Breast Cancer Therapeutics : Implication of Gamma Delta T Cells. *Medicine, Biology*.

(2024). *Breast Cancer Facts and Statistics*. American Cancer Society. Retrieved from https://www.cancer.org/content/dam/cancer-org/research/cancer-facts-and-statistics/annual-cancer-facts-and-figures/2023/2023-cancer-facts-and-figures.pdf

(n.d.). *Breast Cancer Hormone Receptor Status*. American Cancer Society. Retrieved from https://www.cancer.org/cancer/types/breast-cancer/understanding-a-breast-cancer-diagnosis/breast-cancer-hormone-receptor-status.html#:~:text=Breast%20cancer%20cells%20may%20have,positive%20(or%20PR%2B)%20cancers.

Castro, d., K. C., Costa, M., J., Campos, & N, M. G. (2022). Drug-loaded polymeric nanoparticles: a review. *International Journal of Polymeric Materials and Polymeric Biomaterials, 71*(1), 1-13.

Chun-Lan Li, Z.-X. F.-Y.-T. (2022). Repurposed itraconazole for use in the treatment of malignancies as a promising therapeutic strategy. *ELSIVIER*. Retrieved from https://doi.org/10.1016/j.biopha.2022.113616

Chun-Lan, Fang, Z.-X., Wu, Z., Hou, Y.-Y., Wu, H.-T., & Liu, J. (2022). Repurposed itraconazole for use in the treatment of malignancies as a promising therapeutic strategy. *ELSIVIER*. Retrieved from https://doi.org/10.1016/j.biopha.2022.113616

Clarke, M., Collins, R., Darby, S., Davies, C., Elphinstone, P., Evans, V., . . . Wang, Y. (2005). Effects of radiotherapy and of differences in the extent of surgery for early breast cancer on local recurrence and 15-year survival: an overview of the randomised trials. *Lancet, 366*(9506). doi:https://doi.org/10.1016/s0140-6736(05)67887-7

Danhausen, K. E., Phillippi, J. C., & McCance, K. L. (2019). Alterations of the female reproductive system. In Pathophysiology: The biologic basis for disease in adults and children. *St. Louis, MO: Elsevier*(8th ed), 755-834.

Deshmukh, P. R., Joshi, A., Vikhar, C., Khdabadi, S., & Tawar, M. (2022). Current Applications of Chitosan Nanoparticles. *Sys Rev Pharm, 13*(10), 685-693.

Eslam Dabbish, S. S. (2023). *Insights on cyclophosphamide metabolism and anticancer mechanism of action: A computational study*. Retrieved from https://doi.org/10.1002/jcc.27280

Francesco Bertolini, V. P. (2015). Drug repurposing in oncology—patient and health systems opportunities. *Nature Reviews Clinical Oncology*. Retrieved from https://www.nature.com/articles/nrclinonc.2015.169

George, B. P., Chota, A., Sarbadhikary, P., & Abrahamse, H. (2022). Fundamentals and applications of metal nanoparticle-enhanced singlet oxygen generation for improved cancer photodynamic therapy. *Sec. Nanoscience, 10*. doi:https://doi.org/10.3389/fchem.2022.964674

Gulfam, M., Kim, J.-e., Lee, J. M., Ku, B., Chung, B. H., & Chung, B. G. (2012). Anticancer Drug-Loaded Gliadin Nanoparticles Induce Apoptosis in Breast Cancer Cells. *Langmuir, 28*, 8216-8223. doi:dx.doi.org/10.1021/la300691n

Hassanpour, S. H. (2017). Review of cancer from perspective of. *Journal of Cancer Research and Practice, 4*(4), 127-129.

Hegde, P. S., & Chen, D. S. (2020). Top 10 challenges in cancer immunotherapy. *Immunity, 52*(1), 17-35.

Henrich, N. &. (2007). *Why humans cooperate: A cultural and evolutionary explaination.* Oxford University Press.

Hoadley, K. A., Yau, C., Hinoue, T., Wolf, D. M., Lazar, A. J., Drill, E., . . . Thorsson, V. (2016). Cell-of-origin patterns dominate the molecular classification of 10,000 tumors from 33 types of cancer. *Cell, 173*(2), 291-304.

Hoang, N. H., Thanh, T. L., Sangpueak, R., Treekoon, J., Saengchan, C., Thepbandit, W., . . . Buensanteai1, N. (2022, Feb). Chitosan Nanoparticles-Based Ionic Gelation Method: A Promising Candidate for Plant Disease Management. *Polymers, 14*(4), 662. doi:10.3390/polym14040662

Horwitz, K. B., Costlow, M. E., & McGuire, W. L. (1975). MCF-7; a human breast cancer cell line with estrogen, androgen, progesterone, and glucocorticoid receptors. *26*(6), 785-95. doi:10.1016/0039-128x(75)90110-5.

Javad Sharifi-Rad, C. Q. (2021). *Chitosan nanoparticles as a promising tool in nanomedicine with particular emphasis on oncological treatment.* (Cancer Cell Int 21 ed.). Cancer Cell Int 21. Retrieved from https://doi.org/10.1186/s12935-021-02025-4

Jiang M, W. W. (2020). *Protective Effects and Possible Mechanisms of Actions of Bushen Cuyun Recipe on Diminished Ovarian Reserve Induced by Cyclophosphamide in Rats.* Front Pharmaco. Retrieved from https://doi.org/10.3389/fphar.2020.00546

Johns Hopkins Medicine Pathology. (n.d.). Retrieved from https://pathology.jhu.edu/breast/staging-grade/

Jonaid Ahmad Malik, S. A., Jan, B., Bender, O., Hagbani, T. A., Alqarni, A., & Anwar, S. (2022, January). Drugs repurposed: An advanced step towards the treatment of breast cancer and associated challenges. *Elsevier: Biomedicine & Pharmacotherapy, 145*, 112375. doi:https://doi.org/10.1016/j.biopha.2021.112375

Kumar, S., Shaikh, A. J., Rashid, Y. A., Masood, N., Mohammed, A., Malik, U. Z., . . . Khan, S. (2016). Presenting features, treatment patterns and outcomes of patients with breast cancer in Pakistan: Experience at a university hospital. *Indian J Cancer, 53*(2), 230-234. doi:doi: 10.4103/0019-509X.197728.

La-Beck, A. G. (n.d.). Texas Tech University Health Sciences Center.

Liu, F., Gu, L.-N., Shan, B.-E., & Sang, C.-Z. G.-X. (2016). Biomarkers for EMT and MET in breast cancer: An update. *Spandidos Publications*, 4869-4876. doi:https://doi.org/10.3892/ol.2016.5369

Liyanage, P. Y., Hettiarachchi, S. D., Zhou, Y., Ouhtit, A., Seven, E. S., Oztan, C. Y., . . . Leblanc, R. M. (2019). Nanoparticle-mediated targeted drug delivery for breast cancer treatment. *Elsevier, 1871*(2), 413-423. doi:https://doi.org/10.1016/j.bbcan.2019.04.006

Mahmoud, K., Swidan, S., El-Nabarawi, M., & Teaima, M. (2022, March). Lipid based nanoparticles as a novel treatment modality for hepatocellular carcinoma: a comprehensive review on targeting and recent advances. *Journal of Nanobiotechnology volume*.

Makadia, H. K., & Siegel, S. J. (2011). Poly lactic-co-glycolic acid (PLGA) as biodegradable controlled drug delivery carrier. *Polymers, 3*(3), 1377-1397.

Miller, K. D., Siegel, R. L., Lin, C. C., Mariotto, A. B., Kramer, J. L., Rowland, J. H., . . . Jemal, A. (2016). Cancer treatment and survivorship statistics, 2106. *CA: a cancer journal for clinicians*, 271-269.

Mohanraj, V., & Chen, Y. (2006). Nanoparticles-a review. *Tropical journal of pharmaceutical research, 5*(1), 561-573.

Nava-Arzaluz, M. G., Piñón-Segundo, E., Ganem-Rondero, A., & Lechuga-Ballesteros, D. (2012, AUG). Single emulsion-solvent evaporation technique and modifications for the preparation of pharmaceutical polymeric nanoparticles. *Recent patents on drug delivery & formulation, 6*(3), 209-23. doi:10.2174/187221112802652633

Navya, P. N., Kaphle, A., Srinivas, S. P., Bhargava, S. K., Rotello, V. M., & Daima, H. K. (2019). Current trends and challenges in cancer management and therapy using designer nanomaterials. *Nano Convergence*.

(2013). *NCCN Clinical Practice Guidelines in Oncology*. National Comprehensive Cancer Network. Retrieved from http://www.nccn.org/professionals/physician_gls/pdf/breast.pdfAccessed:December 8,2013

NIH consensus conference. (1991). *Treatment of early-stage breast cancer.* JAMA.

Oehler, J. B., Rajapaksha, W., & Albrecht, H. (2024). Emerging Applications of Nanoparticles in the Diagnosis and Treatment of Breast Cancer. *Journal of Personalized Medicine, 14*(7), 723. doi: https://doi.org/10.3390/jpm14070723

Ogino, M. H., & Tadi, P. (2023). Retrieved from https://www.sciencedirect.com/science/article/pii/S0753332222010058#:~:text=Itraconazole%20can%20induce%20the%20apoptosis,death%20in%20various%20cancer%20types.

Pantziarka, P., Sukhatme, V., Bouche, G., & Lydie Meheus, V. P. (2015). Repurposing Drugs in Oncology (ReDO)—itraconazole as an anti-cancer agent. *ecancer medical science*. doi:https://doi.org/10.3332/ecancer.2015.521

Pounds, R., Leonard, S., & Christopher Dawson, S. K. (2017). Repurposing itraconazole for the treatment of cancer (Review). *Oncology Letters*, 2587-2597. doi: https://doi.org/10.3892/ol.2017.6569

Rahman, M., Souto, E. B., Alam, K., & Beg, S. (2021). Liposomal nanotherapeutics in cancer treatment in Nanoformulation Strategies for Cancer Treatment. *Elsevier*, 121-129.

Rao, J. P., & Geckeler, K. E. (2021). Polymer nanoparticles: Preparation techniques and. *Progress in polymer science, 36*(7), 887-913.

S.S.Agrawal, & Sharma, P. (2017). Anticancer Activity of Cyclophosphamide Nanoparticles against Ehrlich Ascites Carcinoma Cells Bearing Swiss Albino Mice. *International Journal of Pharmacy and Pharmaceutical Research, 9*(3).

Saeed, S., Khan, J. A., Iqbal, N., Irfan, S., Shafique, A., & Awan, S. (2019). Cancer and how the patients see it; prevalence and perception of risk factors: a cross-sectional survey from a tertiary care centre of Karachi, Pakistan. *BMC Public Health, 19*.

Schottenfeld, D., & Fraumeni Jr, J. F. (2006). *Cancer epidemiology and prevention.* Oxford University Press.

Shah, R., Rosso, K., & Nathanson, S. D. (2013). Pathogenesis, prevention, diagnosis and treatment of breast cancer. *World Journal of Clinical Oncology, 5*(3), 283-298. doi:https://doi.org/10.5306%2Fwjco.v5.i3.283

Sharma, G. N., Dave, R., Sanadya, J., Piush, & Sharma, K. K. (2010, Apr-Jun). VARIOUS TYPES AND MANAGEMENT OF BREAST CANCER. *Journal of advanced Pharmaceutical Technology and Research, 1*(2), 109-126.

Shreelaxmi Gavas, S. Q. (2021). Nanoparticles for Cancer Therapy: Current Progress and Challenges. *Pubmed Central*. doi:10.1186/s11671-021-03628-6

SKMH. (2018). *Breast Cancer Awareness by Shaukat Khanum Hospital.* doi:https://shaukatkhanum.org.pk/about-us/blog/breast-cancer-awareness-by-shaukat-khanum-hospital

Solanki, G., Shah, N., Chauhan, S., Aundhia, C., Javia, A., & A.K.Seth. (2015). FORMULATION AND EVALUATION OF CYCLOPHOSPHAMIDE LOADED CHITOSAN NANOPARTICLES CONJUGATED WITH FOLIC ACID FOR CANCER TARGETING. *INTERNATIONAL JOURNAL OF PHARMACEUTICAL SCIENCES, 6*(1).

Tsubamoto, H., Ueda, T., Inoue, K., Sakata, K., Shibahara, H., & Sonoda, T. (2017). Repurposing itraconazole as an anticancer agent. *Oncol Lett, 14*(2), 1240-1246. doi:10.3892/ol.2017.6325

Turner, N. C., & Jones, A. L. (2008, July). Management of breast cancer—Part I. *PubMed Central, 337*(7661), 107–110. doi:10.1136/bmj.a421

VARIOUS TYPES AND MANAGEMENT OF BREAST CANCER: AN OVERVIEW. (2010). *Journal of Advanced Pharmaceutical Technology & Research, 1*(2), 109-126.

Wei, X., & Yang, M. (2023). Cell- and subcellular organelle-targeting nanoparticle-mediated breast cancer therapy. *Front Pharmacol, 14*. doi:https://doi.org/10.3389/fphar.2023.1180794

Weinberg, R. A. (1996). How cancer arises. *Sci Am, 275*(3), 62-70. doi:https://doi.org/10.1038/scientificamerican0996-62

Whelan, T., MacKenzie, R., Julian, J., Levine, M., Shelley, W., Grimard, L., . . . Szechtman, B. (2002, August). Randomized trial of breast irradiation schedules after lumpectomy for women with lymph node-negative breast cancer. *Journal of National Cancer Institute, 94*(15), 1143-50. doi:10.1093/jnci/94.15.1143.

WHO. (2022). *Cancer.* Retrieved from https://www.who.int/news-room/fact-sheets/detail/cancer

Winslow, T. (2012). *Ductal Carcinoma In Situ.* National Cancer Institute. Retrieved from https://visualsonline.cancer.gov/details.cfm?imageid=9313

X Wang, S. W. (2017). Anti-proliferation of breast cancer cells with itraconazole: Hedgehog pathway inhibition induces apoptosis and autophagic cell death. *Elsevier*.

Yadav, A., Nisha, & Coskunuzer, B. (2018). Diagnosis of Breast Cancer using Machine Learning Techniques. *Elsevier*.

Yedi Herdiana, N. W. (2023). *Chitosan-Based Nano-Smart Drug Delivery System in Breast Cancer Therapy.* Retrieved from https://www.ncbi.nlm.nih.gov/pmc/articles/PMC10051865/

Yoo, K. Y., & Shin, H. R. (2003). Cancer epidemiology and prevention. *Korean Journal of Epidemiology*, 1-15.

Zielińska, A., Carreiró, F., Ana M. Oliveira, A. N., Pires, B., Venkatesh, D. N., Durazzo, A., . . . Souto, E. B. (2020). Polymeric Nanoparticles: Production, Characterization, Toxicology and Ecotoxicology. *Molecules, 25*(16), 3731. doi:10.3390/molecules25163731